Muonium spectroscopy in ZnSe: Metastability and conversion

R. C. Vilão,* H. V. Alberto, J. Piroto Duarte, J. M. Gil, A. Weidinger, and N. Ayres de Campos
Physics Department, University of Coimbra, P-3004-516 Coimbra, Portugal

R. L. Lichti
Physics Department, Texas Tech University, Lubbock, Texas 79409-1051, USA

K. H. Chow
Department of Physics, University of Alberta, Edmonton, Canada T6G 2J1

S. F. J. Cox
ISIS Facility, Rutherford Appleton Laboratory, Chilton, Didcot, Oxon OX11 0QX, United Kingdom
and Condensed Matter Physics, University College London, WC1E 6BT, United Kingdom
(Received 7 July 2005; revised manuscript received 14 September 2005; published 14 December 2005)

High-precision spectroscopic information is obtained on the muonium states in ZnSe by high-field transverse μSR measurements. At low temperatures, two muonium states Mu_I and Mu_{II} are observed with isotropic hyperfine parameters of $A_I = 3283.63 \pm 0.51$ MHz and $A_{II} = 3454.26 \pm 0.02$ MHz (74% and 77% of the vacuum value, respectively). State I is thermally unstable and converts to state II at approximately 40 K. State II is stable up to 300 K, at least. We assign Mu_{II} to the cation interstitial tetrahedral site and discuss the possibility that Mu_I may correspond either to muonium at the same site but in the unrelaxed lattice or to the anion interstitial tetrahedral site. The temperature dependence of the hyperfine interaction was fitted with a local vibrational model giving an oscillator energy of approximately 8 meV. The amplitudes and the depolarization rates are measured over the entire temperature range and are discussed in the text.

DOI: 10.1103/PhysRevB.72.235203 PACS number(s): 61.72.Vv, 71.55.Gs, 76.75.+i

I. INTRODUCTION

Muonium, consisting of a positive muon and a bound electron, can be considered as a light isotope of hydrogen and can be used to study the properties of hydrogen-related defects in semiconductors.[1,2] Of note, a hydrogenic, i.e., effective mass, donor state was located via muonium spectroscopy in CdS and ZnO[3,4] and has also been seen in several other compounds.[5–9] The shallow donor state in ZnO was subsequently confirmed by IR and electron paramagnetic resonance (EPR)/electron-nuclear double resonance (ENDOR) studies on hydrogen in the same material.[10–12]

In theoretical papers on this subject,[13,14] a systematic behavior of hydrogen defect states over a larger class of semiconductors was reported on. The main prediction is that the stability of the shallow hydrogen donor state depends on the bottom of the conduction band being below a fixed level of about 4.5 eV with respect to the vacuum. This distinguishing level appears to remain constant for a wide range of materials.

ZnSe is, together with ZnO, a prominent representative of the wide band gap II-VI semiconductors, which are under intensive research for potential use in electronic and optoelectronic devices.[15] Unlike ZnO, ZnSe is an example of the second class of compounds, in which the effective mass donor does not occur but instead a deep-level muonium configuration is observed. This is consistent with the predicted amphoteric behavior of hydrogen in ZnSe.[16] The existence of this deep defect state in ZnSe is known from earlier experiments,[17,18] but the spectroscopic information is to date rather scarce because of the small amplitude of the signal. The earlier measurements were made only below about 50 K and did not show that the second atomiclike muonium state, observed in the current experiment, is also present at low temperatures.

The current experiments were performed at high external magnetic field ($\sim$7 T) where precise information on the frequencies and linewidths can be obtained. The primary information from the present study is that a second muonium state exists in ZnSe at low temperature. This state was not seen in the earlier experiments because its linewidth increases with decreasing field and becomes so large at low fields that the spin precession signal is unobservable.

The hyperfine parameters of this second muonium center are very similar to those of the previously known state. Both have an isotropic hyperfine interaction that is a significant fraction of the vacuum value (74% and 77%). A difference is that the muonium state, which we label as Mu_I, becomes unstable with increasing temperature and converts to Mu_{II} at about 40 K. A detailed study of the muonium signals was performed in the temperature range between 2 and 300 K, with emphasis on the conversion region.

II. EXPERIMENTAL DETAILS

ZnSe single crystals obtained commercially (from Alpha-Aesar and from Crystec) were used. The crystals are nominally undoped and cut on the main crystallographic orientations [100], [110], and [111]. The Alpha-Aesar sample was used in the temperature dependence study and the Crystec samples in the orientation dependence study.

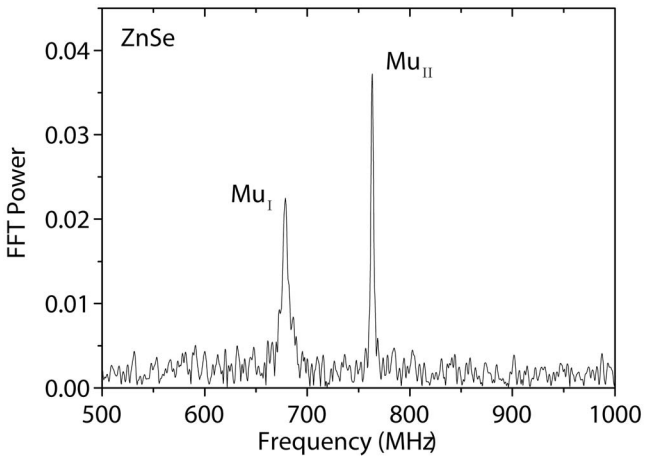

FIG. 1. Fourier transform μSR spectrum of ZnSe at $B=7$ T, and $T=2.07$ K. Two different states, Mu_I and Mu_{II}, are observed. The two lines correspond to distinct muonium centers with two different isotropic hyperfine interactions.

Muon spin rotation (μSR) experiments were performed using the HITIME (high-field, high time resolution) spectrometer in the M15 beam line at TRIUMF, in Vancouver, Canada. These experiments consist of implanting 4 MeV 100% spin-polarized muons into the sample and observing the resulting muon spin precession signals in an external magnetic field that is applied in a direction perpendicular to the initial muon spin polarization.

During the thermalization process, the muon may eventually capture an electron, forming muonium. The muon spin will then precess in the effective field determined by the external field and the hyperfine interaction with the electron. Muons decay with a lifetime of 2.2 microseconds into positrons and undetected neutrinos. Positrons are preferentially emitted in the muon spin direction. Hence, by detecting the emitted positrons as a function of time in various directions, the time evolution of the muon spin polarization can be monitored.

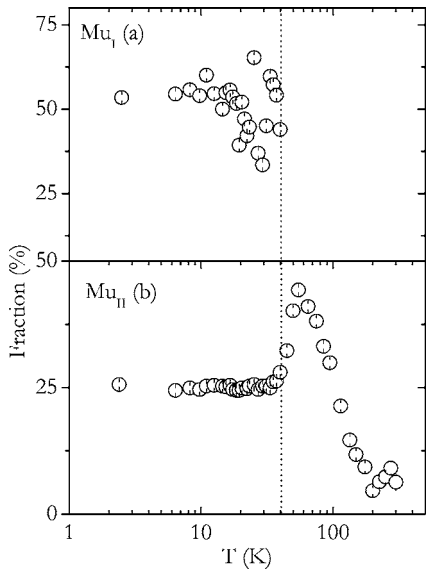

FIG. 2. Fractions of the two muonium states, Mu_I (a) and Mu_{II} (b), as a function of temperature. Mu_I is seen only up to approximately 40 K. Errors as obtained by the fitting program are shown. Systematic errors due to correlation effects are larger and are responsible for the large scattering of the data of Mu_I.

The positron counts in four detectors, arranged in a box-like configuration around the sample, were analyzed in the rotating reference frame. Each frequency signal was analyzed using an exponentially-damped cosine function of the form $A\exp(-\lambda t)\cos(\omega t+\phi)$. The fractions of the two states compared to all muons were calculated from the measured μSR amplitudes assuming that only half of the weight is expected in the observed ν_{12} transition, the second half being contained in the unobserved higher-frequency ν_{34} transition. These frequencies correspond to muon spin "flipping" while the electron spin is up or down, respectively. Instrumental effects that lead to a decrease in the amplitude of the signals at high fields are corrected by comparing with the muon precession signal in silver at the same frequency. The decrease in amplitude for the highest frequency signals due to spectrometer resolution was adjusted according to a calibration of the maximum observable asymmetry using silver.

III. EXPERIMENTAL RESULTS

Figure 1 shows a Fourier transform μSR spectrum in a transverse magnetic field of 7 T at 2 K. At this high field, only the ν_{12} transition in muonium is observable in the experimentally accessible range. Thus the two lines indicate either two distinct muonium centers with different isotropic hyperfine interactions or a single muonium center with an anisotropic hyperfine interaction. In the latter situation, the two lines could arise from different angles between the applied field and the symmetry axis of the hyperfine interaction. We find that the hyperfine frequencies are independent, within experimental errors, of the direction between the applied field and the three major crystallographic directions [100], [110], and [111]. We therefore conclude that two distinct Mu centers, Mu_I and Mu_{II}, with different isotropic hyperfine interactions are responsible for the observed spectra. From the value of the frequencies, we estimate the corresponding values of the hyperfine interactions to be $A_I=3283.63\pm0.51$ MHz and $A_{II}=3454.26\pm0.02$ MHz.

Figure 2 shows the fractions of the two states as a function of temperature. Up to 40 K, both states coexist, Mu_I being nearly twice as intense as Mu_{II}, and the total muonium fraction being $79\pm1\%$. Above 40 K, Mu_I disappears and the fraction of Mu_{II} increases strongly in a narrow temperature interval. This indicates a conversion of Mu_I to Mu_{II}, the latter being the only state visible at higher temperatures. The total intensity of visible muonium signals decreases strongly above the conversion region. This probably is an effect of muon spin depolarization during the time between implantation and formation of the final state, since no appreciable change in the diamagnetic signal (i.e., the signal at the Larmor frequency from muons thermalizing without picking up an electron) is observed in the entire temperature range. The diamagnetic signal strength is extremely small and consistent with the zero diamagnetic fraction arising from the ZnSe

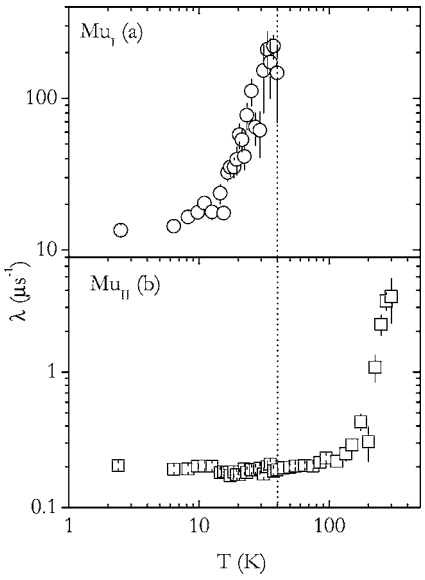

FIG. 3. Depolarization rates of the two muonium states, Mu_I (a) and Mu_{II} (b), as a function of temperature. The pronounced increase of the relaxation of Mu_I is a sign of conversion dynamics, as discussed in the text. The process leading to the increase of relaxation of Mu_{II} is still not understood.

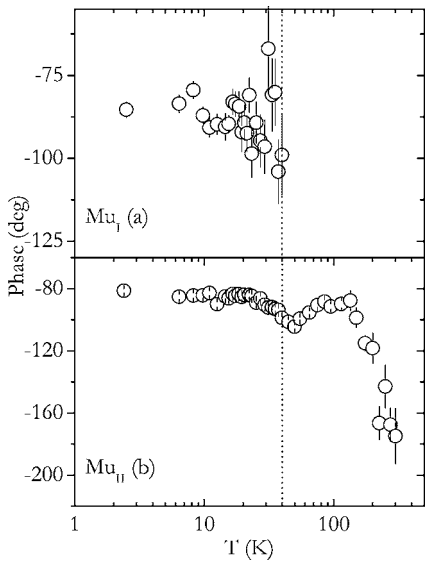

FIG. 4. Phases of the two muonium states, Mu_I (a) and Mu_{II} (b), as a function of temperature. The dip in the phase of Mu_{II} about 50 K is a sign of the conversion dynamics.

sample. This signal can probably be entirely accounted for by muons stopping outside the sample, at all temperatures below 300 K. We will discuss this in more detail below.

The temperature dependence of the depolarization rates λ of the two states can be seen in Fig. 3. The most obvious feature is the strong increase of λ for Mu_I between 10 and 40 K. This is attributed to the temperature activated conversion of state I to state II. The relaxation of Mu_I is also rather large (about 14 μs^{-1}) before the onset of the conversion process perhaps due to a rapid spin fluctuation of Mu_I. The relaxation of state Mu_{II} is very low and does not change up to approximately 200 K, which includes the region of the conversion of state I to state II. Above 200 K an increase of the depolarization of Mu_{II} is seen.

The phases of the signals in each detector are governed by the detector geometry with respect to the muon spin polarization prior to implantation. However, additional phase shifts are introduced if the muon exists for some time in a precursor state before it forms the final configuration.[19] Such phase shift effects are seen in Fig. 4 for Mu_{II} as a dip around 50 K and as the gradual decrease above 100 K.

IV. TEMPERATURE DEPENDENCE OF A_{iso}

We begin to discuss these results in more detail by addressing the temperature dependence of the hyperfine interaction A_{iso} for Mu_{II}, as shown in Fig. 5. Such data are often modelled assuming an interaction with long wavelength phonons which are treated within the Debye model.[19] In the present case the fit to this model gives a Debye temperature of $T_D = 160$ K. The Debye temperature for the ZnSe matrix from the literature is 275 K.[20] Similar discrepancies in a ratio of roughly 2 to 3, were also found for several other semiconductors.[19,21] However, the fit with the Debye model is rather poor for the high temperature points in the current case.

A different approach to the problem is to assign the temperature dependence to a local vibrational mode (e.g., the oscillation of muonium in the potential provided by the matrix) and assume that the change of the hyperfine interaction is adequately described by a series on the mean square displacement $\langle u^2 \rangle$

$$A(T) = a_0 + a_2\langle u^2 \rangle + a_4\langle u^4 \rangle + \cdots . \quad (1)$$

Within this harmonic oscillator model, the temperature dependence can be obtained from a Boltzmann distribution. With the additional assumption that only the vibrational ground state is relevant here, one arrives at the following

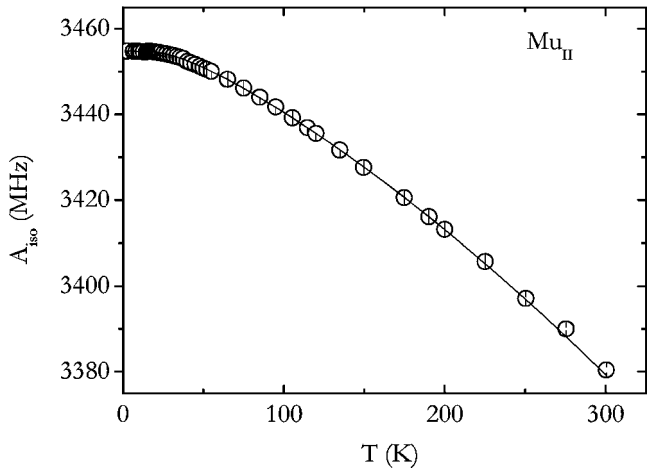

FIG. 5. Temperature dependence of the isotropic hyperfine interaction A_{iso} of state Mu_{II}. The solid line is a fit with an Einstein model, as described in the text, with a vibrational energy of 8 meV.

formula for the temperature dependent isotropic hyperfine interaction $A(T)$:

$$A(T) = A_0 + \frac{C_1}{\exp(h\nu/kT)} + \frac{C_2}{[\exp(h\nu/kT)]^2}, \qquad (2)$$

where A_0 is the hyperfine interaction at $T=0$ K and ν is the single vibration frequency in an Einstein model. The coupling constants C_1 and C_2 are assumed temperature-independent. Equation (2) corresponds to the first three terms of the formula given in Refs. 22 and 23. Without the second order term, a fit with this model did not describe well the data points at the higher temperatures in Fig. 5, indicating a deviation from the simple proportionality between A and $\langle u^2 \rangle$.

The fit (solid line in Fig. 5) gives an energy $h\nu = 8.0 \pm 0.1$ meV. Such a low vibrational energy, if attributed to the oscillation of muonium in the cage, would correspond to an extremely flat potential.

The limited temperature range for observation of Mu_I does not allow any detailed determination of the temperature dependence of the respective hyperfine interaction.

V. Mu_I TO Mu_{II} CONVERSION

A second important aspect in our experimental data relates to the conversion of Mu_I to Mu_{II}. The conversion of an initial state, after some lifetime, to a final state gives rise to a change in the precession frequency. If the initial state lives long compared to the observation time, only the spin precession of the initial state is observed. In the other extreme of a short lifetime, one sees only the precession of the final state, but some effects of the precursor state might still be detectable as a phase shift or a reduction in amplitude. Since the lifetime often depends on temperature, one may observe a transition from one extreme to the other as a function of temperature.

A general treatment of the spin precession in the conversion region is given in Ref. 24. In the present high-field case, the simple one-dimensional formula as given, e.g., in Refs. 25 and 26 can be applied. The polarization change $\Delta P(t)$ is, for the case where state I, detected via frequency ω_I, converts to a state II, which is detected via frequency ω_{II}

$$\Delta P(t) = A_I \exp(-t/\tau)\cos(\omega_I t + \phi_I) + \frac{A_I}{\sqrt{1+(\Delta\omega\tau)^2}} \cos[\omega_{II} t + \phi_I - \tan^{-1}(\Delta\omega\tau)] - \frac{A_I \exp(-t/\tau)}{\sqrt{1+(\Delta\omega\tau)^2}} \cos[\omega_I t + \phi_I - \tan^{-1}(\Delta\omega\tau)], \qquad (3)$$

where τ is the mean lifetime of the initial state and $\Delta\omega = \omega_{II} - \omega_I > 0$. The first term in Eq. (2) represents the relaxation of component I with the rate τ^{-1} corresponding to the lifetime of the state, the third term being a correction to that component with the same relaxation rate τ^{-1}. The second term gives the increase of the amplitude of component II due to the conversion. The amplitude, if not relaxing otherwise, is constant and depends critically on the product $\Delta\omega\tau$. The conversion introduces a phase shift that also depends on $\Delta\omega\tau$. For τ an Arrhenius ansatz $\tau = \tau_{inf} \exp(E_a/kT)$ was used, with E_a the activation energy.

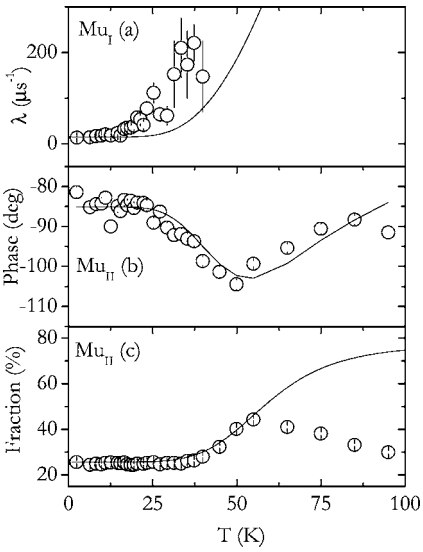

FIG. 6. Relaxation rate of Mu_I, amplitude of Mu_{II}, and phase shift of Mu as a function of temperature. The solid line is a fit to the data with the conversion model and an adjustment of the parameters to the fraction and phase of Mu_{II}. The overestimation of the fraction in Fig. 6(c) above 60 K is due to a reduction of the total muonium formation probability in this temperature range which is not taken into account in the model. The deviation of the data points in Fig. 6(a) from the solid line is attributed to a pre-conversion dynamics leading to an increase of the relaxation (see text).

An acceptable global fit of all data using a unique set of parameters for the conversion could not be obtained. The increase of the relaxation of Mu_I and the rise of the fraction of Mu_{II} (Fig. 6) are too far separated in temperature to be fitted with a single activated conversion process. A similar discrepancy was observed for the conversion of Mu_I to Mu_{II} in CuCl and CuBr.[26] The reason is probably in the stage before the actual conversion, where local motion of muonium and of the lattice atoms may change dramatically and result in an increase of the spin relaxation.

In Figs. 6(b) and 6(c), the solid lines show the fit to the data with the parameters adjusted to the amplitude and phase of Mu_{II}. In the fit we assumed that the amplitudes of Mu_I and Mu_{II} do not change in the conversion temperature range and that their values are the same as at low temperatures. This, however, is not completely correct and leads to the overestimation of the Mu_{II} fraction above 60 K in Fig. 6(c). From this fit, we obtain $E_a = 17$ meV and $\tau_{inf} = 1.1 \times 10^{-4}$ μs. These values should be considered as a first approximation for the Mu_I to Mu_{II} transition, since any other dynamic process involving either state has been left out of this simple model. With the same parameters as in Figs. 6(b) and 6(c), the solid line in Fig. 6(a) is calculated. The discrepancy indicates again that the conversion process is more intricate than assumed in our model. The possible existence of pre-conversion dynamics, as discussed above, may justify the difference.

VI. "MISSING FRACTION"

At low temperatures, ~21% of the muons are not observed in the high transverse-field. However, an extremely fast relaxation of approximately the same amplitude is observed in longitudinal-field depolarization measurements. The observed relaxation rates are field dependent and higher than 100 MHz at 5 K. Once more this indicates the existence of precursor dynamics still to be clarified.

Figures 2 and 6 show that the total muonium fraction, above 60 K represented by the fraction Mu_{II}, decreases with temperature. As pointed out above, no corresponding change is observed in the diamagnetic fraction. A possible explanation for the "missing fraction" is that the donor electrons of ZnSe, which become activated[27] at around 60 K, cause a depolarization of the muon spin in a precursor stage during the thermalization process, i.e., in the time between the implantation and the formation of the final state.

As indicated in Figs. 3 and 4, there is a dramatic change in the relaxation and phase of the Mu_{II} signal above about 200 K. Furthermore, the muonium fraction becomes temperature independent. Above this temperature, donor ionization is essentially complete and any process that depends critically on conduction electron concentration begins to saturate. We note that a conversion from a precursor stage cannot lead to an increase in the relaxation of the final state. Therefore, the increase of the depolarization of Mu_{II} above 200 K (Fig. 3) must be due to a process acting on Mu_{II} directly. It is also unlikely that the increase of the relaxation is due to the onset of a conversion of this state to another state since, in another experiment, Mu_{II} was observed up to 550 K. This observation is not consistent with an activated conversion setting in already at 200 K. Additionally, the observed change in the phase of Mu_{II} above 150 K (Fig. 4) is not related to the Mu_I to Mu_{II} conversion since that transition has become very rapid well below that temperature. These currently unexplained features require further investigation; however, they imply that additional dynamics are present for both Mu_{II} and a precursor state which is not necessarily Mu_I.

Thus an interaction with conduction electrons might be the cause of the relaxation, but the details are not yet established. The observed change of the phase of Mu_{II} above 150 K (Fig. 4) is not related to the Mu_I to Mu_{II} conversion since this process has ended below this temperature as can be seen in Fig. 6. Thus the phase shift must be caused by some process in the precursor stage.

VII. DISCUSSION AND CONCLUSIONS

We have observed a new muonium state in ZnSe at low temperatures, the presence of which accounts for a large portion of the muon fraction that was missing in previous experiments. The detection of this state was made possible only by the application of a high magnetic field, in which the depolarization of the state is sufficiently slow to allow for its observation.

The two states observed here have characteristics very similar to those reported[26,28,29] for CuCl. In these publications, after a detailed characterization of the local surroundings of muonium, definite site assignments were determined, placing both Mu centers in the tetrahedral cage with Cu nearest neighbors but with different lattice relaxations and different specific locations and motional properties for Mu.

A similar situation may exist for both Mu_I and Mu_{II} in ZnSe. By analogy, we expect both centers to reside in the same region, i.e., in the tetrahedral interstitial cage surrounded by four nearest neighbor Zn ions. In this case, Mu_I corresponds to muonium embedded in the not yet relaxed lattice. It finds potential minima slightly off the center position and tunnels among the different sites. A muonium impurity at an off-center location within the tetrahedral cage should have some anisotropy in its hyperfine interaction. The dynamical effect of tunneling would average out this anisotropy and could explain the rather large field-dependent depolarization of Mu_I discussed above.

In the CuCl analogy, Mu_{II} can be assigned to muonium in the center of the Zn cage after lattice relaxation has occurred in reaction to the presence of the muon. There is apparently a barrier between the two configurations which is overcome thermally in the region where the conversion from Mu_I to Mu_{II} is observed. A separation of singlet and triplet tuneling states for muonium delocalized over four cation-related sites has also been proposed as an explanation for such a barrier.[30]

Another interpretation of the two signals could be that they correspond to two different sites, one to muonium in the anion tetrahedral cage and the other to muonium in the cation tetrahedral cage of ZnSe. In a theoretical paper,[31] isotropic hyperfine interactions of 3333 MHz for Mu in the Zn cage (T_{Zn}) and of 3248 MHz for Mu in the Se cage (T_{Se}) were predicted, which are remarkably close to our experimental values. In this second interpretation, Mu_I would correspond to a deep-donor state at T_{Se}, which supports a neutral and a positively charged muonium center. Mu_{II} is then a deep acceptor state at T_{Zn}, which supports a neutral and a negatively charged center.

In the zinc blende structured II-VI materials, which have considerable ionic character in the bonding, the anion cage becomes competitive with the bond-centered location for both the neutral and positively charged donor states. The strong evidence here for conversion from Mu_I to Mu_{II} would then imply that the T_{Zn} acceptor site is the more stable location for Mu in ZnSe. This experimental evidence also implies that, in the two-site model, the site-change transition is faster than Mu_I ionization below roughly 50 K. However, if the Mu_I deep-donor ionization rate were competitive and increasing more rapidly with temperature, then ionization of Mu_I prior to conversion to Mu_{II} could provide a simple explanation for the decrease in Mu_{II} amplitude that is observed between 60 and 150 K (Fig. 2). This is also consistent with a second exit route from Mu_I as inferred from the fits to the data of Fig. 6.

The present experiment confirms that normal muonium at an acceptor site, here called Mu_{II}, is the stable muon configuration in ZnSe. The only other neutral signal in ZnSe is Mu_I which converts to Mu_{II}. Here, and in many other investigations of ZnSe, no sign of the shallow effective-mass donor has been found. Thus ZnSe belongs to the class of semiconductors in which the shallow donor is absent and instead one or more deep muonium centers are observed, as is the case for Si or for GaAs.[1] There is no clear experimental evidence

in ZnSe, as there was for CuCl, on which to base an independent choice between the two-site and single-site models; thus, it is not definite at this juncture whether or not a deep donor state is also observed in addition to the deep acceptor ground state. However, several arguments favor the single-site model; the Mu_I relaxation rates, the very close resemblance of ZnSe and similarity of the data to the CuCl system, together with the definite assignment of the two Mu signals to the same *T*-site cage in CuCl. All these advocate rather strongly in favor of the single-site interpretation.

ACKNOWLEDGMENTS

The technical help of the μSR facility scientists at TRIUMF is gratefully acknowledged. This work was partially supported by FCT/FEDER European Funds (Grant Nos. POCTI/35334/FIS/2000 and POCTI/43623/FIS/2000-Portugal), by the U.S. National Science Foundation (Grant No. DMR-0102862), and the Welch Foundation (Grant No. D-1321). K.H.C. and TRIUMF are supported by the National Sciences and Engineering Research Council of Canada.

*Electronic address: ruivilao@ci.uc.pt

[1] K. H. Chow, B. Hitti, and R. F. Kiefl, in *Identification of Defects in Semiconductors*, edited by M. Stavola (Academic Press, San Diego, 1998), Vol. 51A, pp. 137–207.
[2] S. K. Estreicher, Mater. Sci. Eng., R. **14**, 319 (1995).
[3] J. M. Gil, H. V. Alberto, R. C. Vilão, J. P. Duarte, P. J. Mendes, L. P. Ferreira, N. Ayres de Campos, A. Weidinger, J. Krauser, Ch. Niedermayer, and S. F. J. Cox, Phys. Rev. Lett. **83**, 5294 (1999).
[4] S. F. J. Cox, E. A. Davis, S. P. Cottrell, P. J. C. King, J. S. Lord, J. M. Gil, H. V. Alberto, R. C. Vilão, J. Piroto Duarte, N. Ayres de Campos, A. Weidinger, R. L. Lichti, and S. J. C. Irvine, Phys. Rev. Lett. **86**, 2601 (2001).
[5] J. M. Gil, H. V. Alberto, R. C. Vilão, J. Piroto Duarte, N. Ayres de Campos, A. Weidinger, J. Krauser, E. A. Davis, S. P. Cottrell, and S. F. J. Cox, Phys. Rev. B **64**, 075205 (2001).
[6] K. Shimomura, R. Kadono, K. Ohishi, M. Mizuta, M. Saito, K. H. Chow, B. Hitti, and R. L. Lichti, Phys. Rev. Lett. **92**, 135505 (2004).
[7] E. A. Davis, S. F. J. Cox, R. L. Lichti, and C. G. Van de Walle, Appl. Phys. Lett. **82**, 592 (2003).
[8] R. C. Vilão, H. V. Alberto, J. M. Gil, J. Piroto Duarte, N. Ayres de Campos, A. Weidinger, and M. V. Yakushev, Physica B **340**, 965 (2003).
[9] S. F. J. Cox, S. P. Cottrell, J. S. Lord, R. C. Vilão, H. V. Alberto, J. Piroto Duarte, J. M. Gil, N. Ayres de Campos, E. A. Davis, M. Charlton, D. P. Van der Werf, D. J. Keeble, R. L. Lichti, and A. Weidinger, AIP Conf. Proc. **772**, 193 (2005).
[10] D. M. Hofmann, A. Hofstaetter, F. Leiter, H. Zhou, F. Henecker, B. K. Meyer, S. B. Orlinskii, J. Schmidt, and P. G. Baranov, Phys. Rev. Lett. **88**, 045504 (2002).
[11] E. V. Lavrov, J. Weber, F. Borrnert, C. G. Van de Walle, and R. Helbig, Phys. Rev. B **66**, 165205 (2002).
[12] M. D. McCluskey, S. J. Jokela, K. K. Zhuravlev, P. J. Simpson, and K. G. Lynn, Appl. Phys. Lett. **81**, 3807 (2002).
[13] C. G. Van de Walle and J. Neugebauer, Nature (London) **423**, 626 (2003).
[14] Ç. Kiliç and A. Zunger, Appl. Phys. Lett. **81**, 73 (2002).
[15] *II-VI Semiconductor Blue/Green Light Emitters*, edited by A. Nurmikko and R. Gunshor (Academic Press, New York, 1997), Vol. 44.
[16] C. G. Van de Walle, Phys. Status Solidi B **229**, 221 (2002).
[17] J. W. Schneider, Hp. Baumeler, H. Keller, R. F. Kiefl, W. Kündig, W. Odermatt, B. D. Patterson, T. L. Estle, S. P. Rudaz, K. W. Blasey, and C. Schwab, Hyperfine Interact. **32**, 607 (1986).
[18] A. Weidinger, H. V. Alberto, J. M. Gil, R. C. Vilão, J. Piroto Duarte, and N. Ayres de Campos, Phys. Status Solidi C **0**, 711 (2003).
[19] B. D. Patterson, Rev. Mod. Phys. **60**, 69 (1988).
[20] J. A. Birch, J. Phys. C **8**, 2043 (1975).
[21] R. L. Lichti, W. A. Nussbaum, and K. H. Chow, Phys. Rev. B **70**, 165204 (2004).
[22] E. Roduner, P. W. Percival, P. Han, and D. Bartels, J. Chem. Phys. **102**, 5989 (1995).
[23] J. R. Morton, F. Negri, and K. F. Preston, Phys. Rev. B **49**, 12446 (1994).
[24] P. F. Meier, Phys. Rev. A **25**, 1287 (1982).
[25] A. Möslang, H. Graf, G. Balzer, E. Recknagel, A. Weidinger, Th. Wichert, and R. I. Grynszpan, Phys. Rev. B **27**, 2674 (1983).
[26] R. F. Kiefl, W. Odermatt, Hp. Baumeler, J. Felber, H. Keller, W. Kündig, P. F. Meier, B. D. Patterson, J. W. Schneider, K. W. Blazey, T. L. Estle, and C. Schwab, Phys. Rev. B **34**, 1474 (1986).
[27] S. S. Devlin, in *Physics and Chemistry of II-VI Compounds*, edited by M. Aven and J. S. Prener (North-Holland, Amsterdam, 1967), p. 597.
[28] J. W. Schneider, H. Keller, W. Odermatt, B. Pümpin, I. M. Savic, H. Simmler, S. A. Dodds, T. L. Estle, R. C. DuVarney, K. Chow, R. Kadono, R. F. Kiefl, Q. Li, T. M. Riseman, H. Zhou, R. L. Lichti, and C. Schwab, Hyperfine Interact. **64**, 543 (1990).
[29] J. W. Schneider, R. F. Kiefl, K. Chow, S. F. J. Cox, S. A. Dodds, R. C. DuVarney, T. L. Estle, R. Kadono, S. R. Kreitzman, R. L. Lichti, and C. Schwab, Phys. Rev. Lett. **68**, 3196 (1992).
[30] S. F. J. Cox, J. Phys. C **20**, 3187 (1987).
[31] C. G. Van de Walle and P. E. Blöchl, Phys. Rev. B **47**, 4244 (1993).